JOURNAL OF MATERIALS SCIENCE 31 (1996) 2401–2407

Mechanism and kinetics of type II discontinuous coarsening in a Zn–4 at % Ag alloy

I. MANNA, J. N. JHA, S. K. PABI
Metallurgical & Materials Engineering Department, Indian Institute of Technology, Kharagpur, W.B. 721302, India

Discontinuous coarsening (DC) may succeed discontinuous precipitation (DP) either at the same (DCI) or another temperature (DCII). The present study concerns mechanism and kinetics of DCII in a Zn–4 at % Ag alloy in the range 353–513 K following DP at 393 K for 60 h. DCII colonies prefer to initiate either from one or both sides of the interfaces between the former DP colonies. A suitable comparison of the kinetic data reveals that interlamellar spacing (λ) and steady-state growth velocity (v) values in DCII are significantly different than those in DP. On the other hand, the kinetics of DCI *vis-à-vis* DCII in terms of λ and v are comparable to each other, though the calculated values of the driving forces between them differ marginally. A detailed kinetic analysis of DCII through the Livingston–Cahn model leads to an underestimation of the activation energy (Q_b) of grain boundary chemical diffusion of Ag in Zn–Ag ($=30.7\ kJ\ mol^{-1}$), whereas the same obtained from the modified Petermann–Hornbogen model ($=61.0\ kJ\ mol^{-1}$) compares well with that for DP/DCI (reported elsewhere by us), and grain boundary self diffusion of Zn. Considering that Q_b in DCII is nearly 50% of the activation energy for volume/matrix diffusion of Ag in Zn, it appears that DCII in the present alloy is a boundary diffusion controlled process.

1. Introduction

Discontinuous coarsening (DC) is a typical moving boundary transformation like discontinuous precipitation (DP) or eutectoid transformation (ET). In DC, the primary transformation products of DP or ET are replaced with a similar but coarser distribution of a two phase aggregate behind a moving boundary (called the reaction front, RF) advancing into a DP/ET colony [1–3]. Livingston and Cahn [4] discovered DC in the products of ET in Co–Si, Cu–In, and Ni–In [2]. Subsequently, DC has been reported to succeed DP in several binary systems in the course of continued isothermal ageing at the same temperature (T) (referred to as type I or DCI), e.g. in Al–Zn [5, 6], Cu–Cd [7], Ni–In [8], Cu–Sb [9] and Cu–Be [10, 11]. Livingston and Cahn [4] assumed that the reactant and product phases in DC had the same compositions, and the driving force for DC was derived solely from the reduction in interfacial free energy (ΔG_γ) accompanying the coarsening reaction. However, the chemical free energy changes (ΔG_c) due to the residual solute supersaturation (ΔX) in the matrix phase, if any, may supplement the driving force for DC. In fact, ΔX is seldom zero immediately following DP [12], and hence, may be relieved in the course of DC succeeding DP at the same T. But it is not necessary that DP and DC should take place at the same T. Shaarbaf and Fournelle [13] studied DC at a T other than that in which DP had occurred (referred to as type II or DCII) in an Al–29 at % Zn alloy. However, a suitable comparison between the growth mechanism and kinetics of that investigation (i.e. DCII) with the relevant data from the DCI studies with the same alloy previously reported in the literature [5, 6] was not attempted. Such a comparison is warranted because the driving force (in terms of both ΔG_c and ΔG_γ) for DCI is not necessarily the same as that in DCII. We have recently reported an investigation on DCI in a Zn–4 at % Ag alloy [14]. In the present paper, we shall report a DCII study with the same alloy to compare the mechanism and kinetics of these two types of moving boundary coarsening reactions (i.e. DCI *vis-à-vis* DCII) under comparable conditions.

2. Experimental procedure

The Zn–4 at % Ag alloy for this investigation was prepared from high purity (>99 wt %) Zn and Ag by vacuum induction melting and casting. The 8 mm diameter cast ingot was homogenized at 683 K for two weeks under vacuum, and quenched in water. Circular discs of about 5 mm in height were cut from the ingot, solution annealed at 683 K for 12 h, and quenched in water at room temperature. The as-quenched samples were aged at 393 K for 60 h to achieve 90% of the DP reaction [14]. This was followed by further ageing between 353–513 K for different periods of time (t) to produce DCII. Samples for metallographic studies were prepared by conventional mechanical polishing with 0.1 μm diamond paste, and etching with

0022–2461 © *1996 Chapman & Hall*

a solution of 1 ml nitric and 1 ml acetic acid in 98 ml distilled water. Optical microscopy (OM) was utilized to determine the growth rate of the DCII colonies and repeat distance of the β phase. The mechanism of initiation and growth of the colonies was carefully monitored by scanning electron microscopy (SEM). An average of the maximum normal distance between the original position of the boundary to its leading edge, measured from 30–50 different colonies, was used to express the average of the maximum colony width ($\bar{w}$). The error in determining the true colony width (w) due to possible differences in orientation of the DCII colonies with respect to the plane of observation was normalized by multiplying $\bar{w}$ with $\pi/4$ [15]. Similar normalization was also carried out to determine the true interlamellar spacing (λ_{DCII}) by multiplying the average of the interlamellar distance $\bar{\lambda}_{DCII}$ (obtained from 20–30 independent measurements from different colonies) with $\pi/4$ [15]. The steady-state RF velocity for DCII (v_{DCII}) was determined from the slope of the variation of w as a function of t under different isothermal conditions, i.e. $v_{DCII} = (dw/dt)_T$.

3. Results and discussion

3.1. Morphology and mechanism

Fig. 1 reveals a typical DP colony comprising a two phase lamellar aggregate of the solute-depleted matrix (α) may precipitate (β) phases, formed at $T = 393$ K after $t = 60$ h. It may be noted that the true interlamellar spacing during DP (λ_{DP}) has been statistically constant. However, orientation of the β-lamellae with respect to the plane of observation, reflected by the difference in lustre, may change within the same colony without affecting λ_{DP} (cf. Fig. 1). It is known that continued ageing at the same T results into DC (i.e. DCI) in this alloy [14]. Similarly, isothermal ageing at another T following DP at 393 K for 60 h leads to DCII with a distinct coarsening of the interlamellar spacing so that $\lambda_{DCII} \gg \lambda_{DP}$. Fig. 2 presents the initial stage of DCII at $T = 433$ K after $t = 40$ h following DP at 393 K for $t = 60$ h. Here, the DCII colony seems to have initiated at the junction of the two former DP colonies. In a previous work [14], DCI colonies were observed to initiate either at the interface between two DP colonies, at a DP-RF, or from within a DCI colony at the point of intersection with the free surface. In contrast, DCII colonies in the present study appear to initiate preferentially from the interfaces between two former DP colonies rather than from the original location of the boundary that initiated a DP colony. It is interesting to note that the width (δ) of the interface that initiated the DCII colony in Fig. 2 is unusually large (≈1–2 μm) compared to the usual δ of a random grain/interphase boundary (i.e. 0.5 nm). In fact, δ of this initiation site is comparable with the average thickness of the β-lamellae in the DCII colony. In an earlier work on a Cu–12 at % In alloy [16], a similar increase in δ was considered a prerequisite for a coherent/semi-coherent interfacial segment to attain an incoherent character to be able to undergo thermally activated migration and initiate DP from the interphase regions. Perhaps, volume/

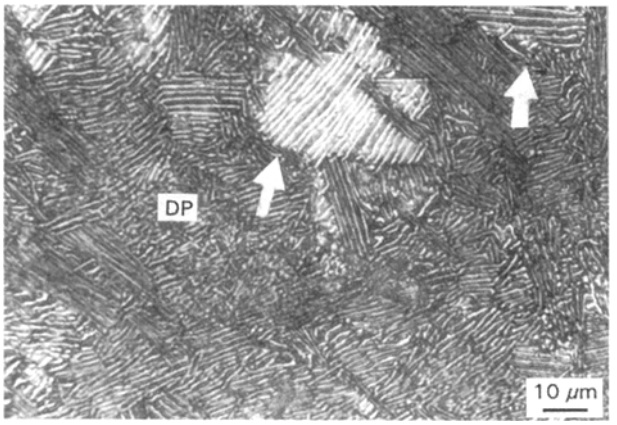

Figure 1 An optical micrograph revealing a typical DP colony comprising a two phase (α + β) lamellar aggregate formed at 393 K after 60 h. The arrowheads indicate localized regions with different orientations of the β-lamallae.

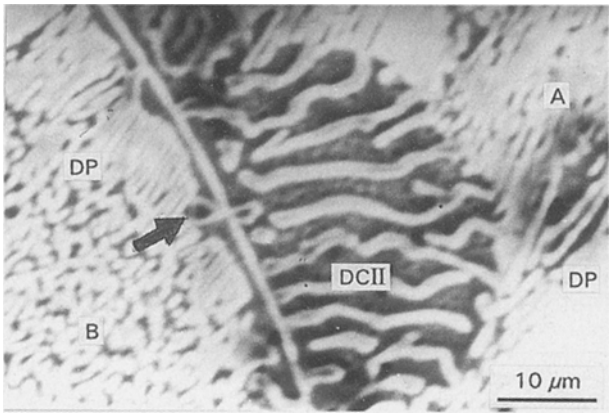

Figure 2 An SEM micrograph showing the growth of a DCII colony (consuming a DP colony, A) formed at 433 K after 40 h following DP at 393 K for 60 h. The greater than usual width of the interface initiating DCII (between two former DP colonies) may be noted. The arrowhead points out a boundary allotriomorph formed across the interface, in DP colony B.

matrix diffusion of the solute atoms (due to the ΔX left in α following DP) towards the nearest interface leads to this increase in δ noted in Fig. 2. A β-rich envelope develops during the coarsening process and it now becomes easier to form boundary allotrimorphs on the other side (Fig. 2) and initiate another DCII colony with an opposite growth-direction. Fig. 3 shows two DCII colonies growing from the same initiation site through the above-mentioned mechanism with opposite directions of growth. It may be noted that the proposed mechanism of growth here is analogous to the formation of the "double-seam" morphology during the isothermal growth of a DP colony [17].

Livingston and Cahn [4] have earlier predicted that DC would initiate at the junction of two DP colonies, and grow from that colony, the primary reaction products in which are parallel to the boundary initiating DC. But evidence in support of such a strict orientation relationship between the primary and secondary reaction products is not forthcoming in the present alloy. Finally, it may be noted that the α and β phases in the DCII colonies appear to be connected with the respective phases in the DP colonies (being consumed) across the RF (Figs 2 and 3).

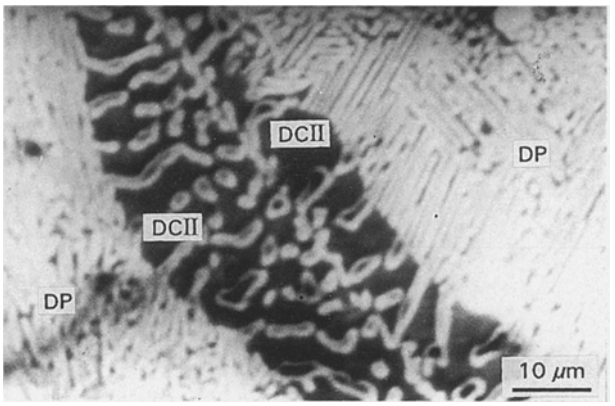

Figure 3 An SEM micrograph illustrating the growth of two DCII colonies in opposite directions away from the same initiation site at 433 K after 40 h following DP at 393 K for 60 h.

3.2. Reaction front migration rate

Fig. 4 illustrates the isothermal variation of w as a function of t at different T. Regression analysis of the respective sets of data reveals a satisfactory linear relationship between w and t in the range of T studied. As mentioned earlier, the slopes of the straight lines in Fig. 4 represents the steady-state RF velocity during DCII (v_{DCII}). Fig. 5 records the variation of v_{DCII} with T. For comparison, a similar variation of the isothermal RF velocities during DP (v_{DP}) and DCI (v_{DCI}) with T, determined in an earlier study [14], are also reported in Fig. 5. Both v_{DCI} and v_{DCII} increase with an increase in T, and v_{DCI} is marginally higher than v_{DCII} at a given T. However, the difference is within experimental scatter. On the other hand, the v_{DP}–T variation registers a typical C-curve behaviour, characteristic of a diffusion controlled nucleation and growth process. It is relevant to mention that DCI/DCII could not be monitored at $T \geqslant 513$ K due to a strong tendency of continuous coarsening at elevated temperatures. Furthermore, v_{DP} is nearly two orders of magnitude higher than v_{DCI} or v_{DCII} at a given T. This difference between the RF migration rates during DP and DCI/DCII seems to be prevalent, at least qualitatively, in all other binary systems known to undergo DP followed by DCI/DCII [5–11, 13, 14]. It is presumed that the difference between v_{DP} and v_{DCI}/v_{DCII} may be attributed to the lower driving force for DCI/DCII compared to DP, especially when ΔG_c for DCI/DCII is not negligible.

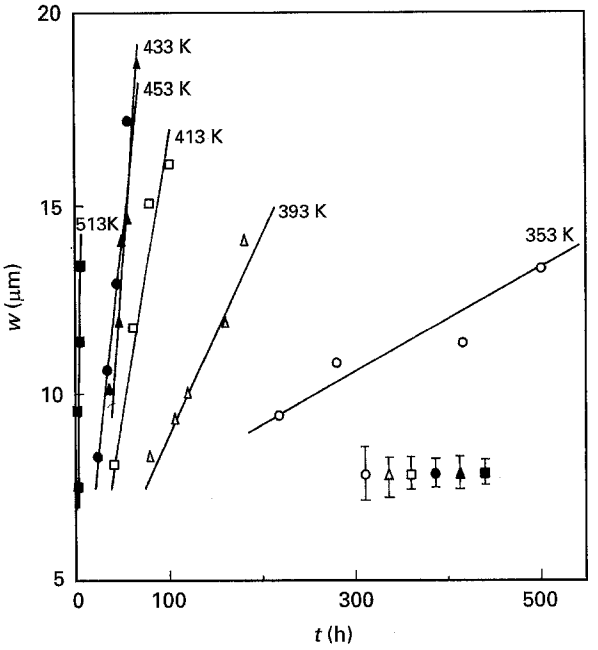

Figure 4 Isothermal variation of w as a function of t at different T. The errors bars indicate the average limits of uncertainty of the respective set of data.

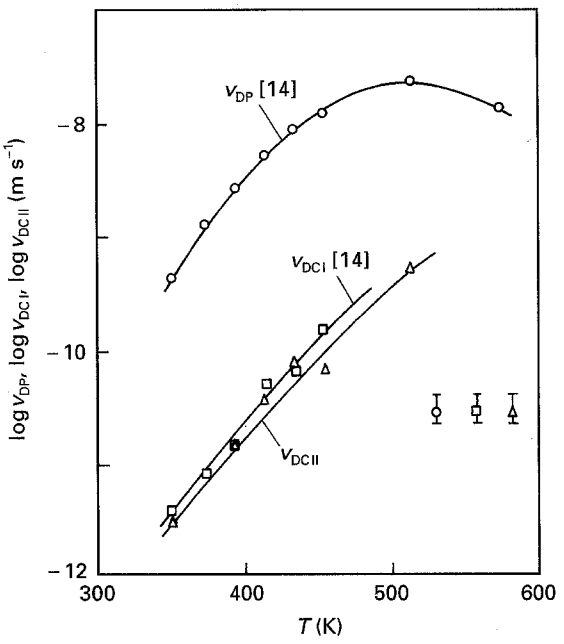

Figure 5 Variation of the velocities in DP (v_{DP}), DCI (v_{DCI}) and DCII (v_{DCII}) as a function of isothermal temperature (T).

3.3. Interlamellar spacing

Fig. 6 presents the variation of λ_{DCII} as a function of T, and compares the same with λ_{DP} and λ_{DCI} (as a function of T), determined in an earlier study [14]. λ_{DCI} records a monotonic increase with an increase in T, while λ_{DCII} follows a similar trend up to 433 K, and levels off thereafter. Earlier, Shaarbaf and Fournelle [13] reported a similar non-systematic variation of λ_{DCII} with T in a DCII study in the Al–Zn system. It is known that interlamellar spacing is closely related to the RF migration rate under isothermal conditions of growth in any moving boundary transformation [2]. However, a direct correspondence of the anomalous temperature dependence of λ_{DCII} is not presentable at this stage due to its complex relationship with the phase chemistry, boundary structure and mobility, etc. However, it should be noted that λ_{DCI} or λ_{DCII} is 4–6 times larger than λ_{DP} at a comparable T. Similarly, $\lambda_{DCI} \gg \lambda_{DP}$ has earlier been reported in a number of other binary systems [5–12]. It is important to note that $\lambda_{DCII} \gg \lambda_{DP}$) in the present study is a result of an independent DC reaction (at a given T), and the difference between λ_{DCII} and λ_{DP} cannot be attributed to the change in isothermal ageing temperature.

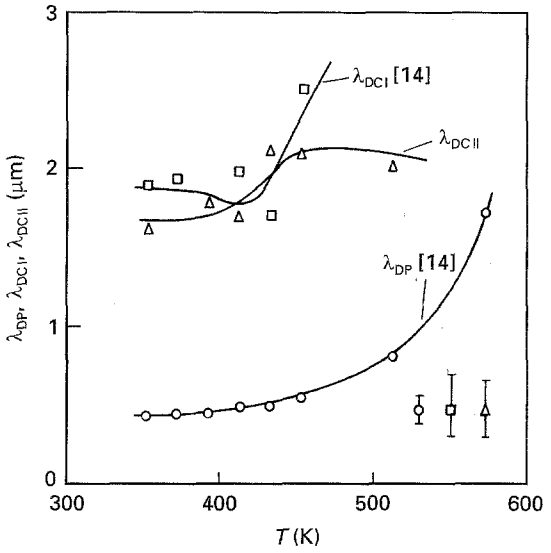

Figure 6 Variation of true interlamellar spacing in DP (λ_{DP}), DCI (λ_{DCI}) and DCII (λ_{DCII}) as a function of isothermal temperature (T).

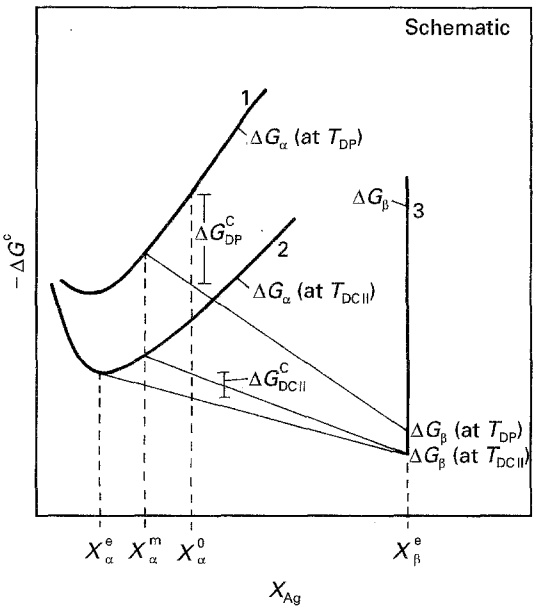

Figure 7 A schematic diagram showing a change in chemical free energy (ΔG^c) with composition (X_{Ag}) and illustrating the principle of determining the chemical free energy change in DCII (ΔG^c_{DCII}) at $T = T_{DCII}$ following DP at $T = T_{DP}$.

3.4. Determination of driving force for DCII

It is known that the average composition of α following DP corresponds to the metastable solvus (X^m_α) (as α is assumed to be in metastable equilibrium with β in a DP colony [18, 19]) such that $X^m_\alpha > X^e_\alpha$ [12], where X^e_α represents the equilibrium–solvus composition. Thus, $\Delta X = (X^m_\alpha - X^e_\alpha)$ at a given T may contribute towards the overall driving force for DCII (ΔG_{DCII}) in the following way [13]:

$$\begin{aligned}\Delta G_{DCII} &= \Delta G^c_{DCII} + (\Delta G^\gamma_{DCII} - \Delta G^\gamma_{DP}) \\ &= (\Delta G^e_{\alpha+\beta} - \Delta G^m_{\alpha+\beta}) + (\Delta G^\gamma_{DCII} - \Delta G^\gamma_{DP})\end{aligned} \quad (1)$$

where $\Delta G^c_{DCII} = \Delta G_c$ in DCII, $\Delta G^\gamma_{DCII} = \Delta G_\gamma$ in DCII, $\Delta G^\gamma_{DP} = \Delta G_\gamma$ in DP, $\Delta G^e_{\alpha+\beta}$ = average ΔG_c associated with DCII, and $\Delta G^m_{\alpha+\beta}$ = average ΔG_c associated with DP, respectively. $\Delta G^e_{\alpha+\beta}$ may be obtained by applying the lever rule as follows:

$$\begin{aligned}\Delta G^e_{\alpha+\beta} &= [(X^e_\beta - X^o_\alpha)/(X^e_\beta - X^e_\alpha)]\Delta G^e_\alpha \\ &\quad + [(X^o_\alpha - X^e_\alpha)/(X^e_\beta - X^e_\alpha)]\Delta G_\beta\end{aligned} \quad (2)$$

where X^o_α and X^e_β are the respective solute contents in the supersaturated (initial) and precipitate phases, and ΔG^e_α and ΔG_β represent the chemical free energy changes of formation of the α and β phases (following DCII), respectively. ΔG^e_α is readily obtained from the regular solution model [3, 20]:

$$\begin{aligned}\Delta G^e_\alpha &= RT[X^e_\alpha \ln X^e_\alpha + (1 - X^e_\alpha)\ln(1 - X^e_\alpha)] \\ &\quad + \Omega RT X^e_\alpha (1 - X^e_\alpha)\end{aligned} \quad (3)$$

where Ω = regular solution function [20], and R = universal gas constant. The required value of Ω for this study is not available in the literature. According to Chuang *et al.* [8], Ω can indirectly be estimated as follows:

$$\Omega = \frac{(\Delta G_\beta/RT) - [X^e_\beta \ln X^e_\alpha + (1 - X^e_\beta)\ln(1 - X^e_\alpha)]}{(X^e_\alpha)^2 + X^e_\beta - 2X^e_\alpha X^e_\beta} \quad (4)$$

Determination of Ω through Equation 4 is subject to the availability of ΔG_β as a function of T. However, ΔG_β is not available in the literature at the required composition and temperature range. Hultgren *et al.* [21] have reported the enthalpy (ΔH_β) and entropy (ΔS_β) changes for the formation of β for a limited range of composition only at $T = 873$ K. Extrapolating the values of ΔH_β and ΔS_β to $X^e_\beta = 0.126$, and assuming them to be temperature independent, ΔG_β may be calculated at the required T. Furthermore, the values of Ω, and consequently ΔG^e_α, may now be estimated as a function of T through Equations 4 and 3, respectively. Subsequently, it is also possible now to determine $\Delta G^e_{\alpha+\beta}$ through Equation 2. Similarly, $\Delta G^m_{\alpha+\beta}$ may be readily obtained through a similar exercise by replacing X^e_α with X^m_α in Equations 2 and 3. It may be noted that X^m_α (=0.0131, obtained from our earlier study [14]) remains constant for calculating $\Delta G^m_{\alpha+\beta}$ in the present DCII study. Fig. 7 schematically illustrates the procedure of determination of ΔG^e_{DCII} at a given $T = T_{DCII}$, when DCII succeeds DP from $T = T_{DP}$.

Now, ΔG^γ_{DCII} is a function of the interfacial energy (γ) of the α–β interfaces, molar volume of the two phase aggregate (V_m) and λ_{DCII} as follows [3]:

$$\Delta G^\gamma_{DCII} = 2\gamma V_m/\lambda_{DCII} \quad (5)$$

Similarly, ΔG^γ_{DP} may be obtained through Equation 5 by replacing λ_{DCII} with $\lambda_{DP} = 0.45$ μm (at 393 K, obtained from a separate study by us on DCI with the same alloy [14]). The value of γ for the Zn–Ag system is not reported in the literature. However, the grain boundary specific energy of pure Zn is 340 mJ m^{-2} at 573 K [22]. Assuming a reduction in γ due to alloying with Ag, it is rational to assign $\gamma = 270$ mJ m^{-2} at 573 K with $d\gamma/dT = -0.1$ mJ m^{-2} K^{-1} for the present alloy. Applying the lever rule, V_m for the ($\alpha + \beta$)

TABLE I Thermodynamic data for calculation of the driving force for DCII (ΔG_{DCII}) following DP at 393 K as a function of T

T (K)	$\Delta G^{m}_{\alpha+\beta}$ (J mol^{-1})	$\Delta G^{e}_{\alpha+\beta}$ (J mol^{-1})	ΔG^{e}_{DCII} (J mol^{-1})	γ (mJ m^{-2})	ΔG^{γ}_{DP} (J mol^{-1})	λ_{DCII} (μm)	ΔG^{γ}_{DCII} (J mol^{-1})	ΔG_{DCII} (J mol^{-1})
353	−993.6	−1014.7	−21.1	292	11.8	1.62	3.3	−29.6
393	−1067.3	−1074.1	−6.8	288	11.6	1.78	2.9	−15.5
413	−1102.3	−1105.0	−2.7	286	11.6	1.70	3.1	−11.1
433	−1135.5	−1136.4	−0.9	284	11.5	2.11	2.4	−10.0
453	−1168.4	−1168.4	0.0	282	11.4	2.10	2.4	−9.0
513	−1271.5	−1282.4	−10.9	276	11.2	2.02	2.5	−19.6

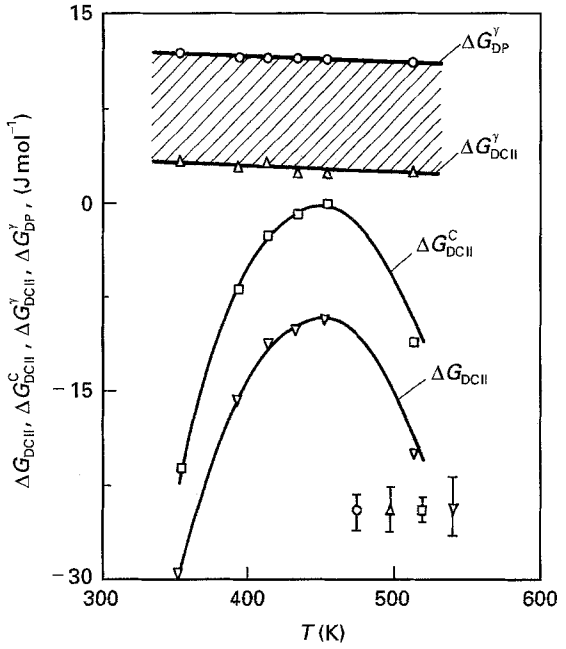

Figure 8 Variation of the overall Gibbs free energy change in DCII (ΔG_{DCII}), with its chemical and interfacial components as a function of T. The hatched portion indicates the change in interfacial free energy in DCII.

aggregate (i.e. DCII colony) in the present alloy has been calculated to be 9.1×10^{-6} m^3 mol^{-1} [14].

Therefore, ΔG_{DCII} may now be calculated as a function of T through Equation 1, the necessary data for which are summarized in Table I. Fig. 8 shows the variation of different components of ΔG_{DCII} as a function of T. It is interesting to note that the curves corresponding to ΔG^{c}_{DCII}, and hence ΔG_{DCII}, undergo a reversal following a peak at $T = 453$ K (where $X^{m}_{\alpha} \simeq X^{e}_{\alpha}$). It is relevant to point out that this behaviour is typical of DCII reactions in comparison to that in DCI. This reversal is absent in DCI because ΔG^{c}_{DCI} is never zero as the solute content in the α-phase following DP is always lower than that of the same phase after DCI.

3.5. Determination of Arrhenius parameters of boundary diffusion

Livingston and Cahn [4] have proposed that the boundary chemical diffusivity triple product ($s\delta D_b$) may be expressed as [13]:

$$s\delta D_b = \frac{v_{DCII}(X^{e}_{\beta} - X^{e}_{\alpha}) f^{2}_{\beta} f^{2}_{\alpha} \lambda^{2}_{DCII} \lambda_{DP} RT}{8 X^{e}_{\alpha}\{1 - (\lambda_{DP}/\lambda_{DCII})\}\gamma V_m} \quad (6)$$

where s is the segregation factor [23], D_b the intrinsic boundary diffusivity, and f_α and f_β the volume fractions of α and β phases, respectively. f_α and f_β may be readily calculated applying the lever rule and using the X^{e}_{α} and X^{e}_{β} values from the Zn–Ag phase diagram [24].

On the other hand, Fournelle [25] modified the Petermann–Hornbogen model on DP [26] as follows:

$$(s\delta D_b) = RTv_{DCII}(\lambda_{DCII})^2/[8(-\Delta G_{DCII})] \quad (7)$$

Table II presents the relevent data for the estimation of ($s\delta D_b$) as a function of T, using Equations 6 and 7.

The temperature dependence of ($s\delta D_b$) may conveniently be expressed through an Arrhenius type of equation [1, 3]:

$$(s\delta D_b) = (s\delta D_b)_o \exp[-Q_b/RT] \quad (8)$$

where $(s\delta D_b)_o$ is the pre-exponential constant, and Q_b is the activation energy of boundary chemical diffusion. Fig. 9 records the Arrhenius plots of ($s\delta D_b$), obtained through Equations 6 and 7. For comparison, similar Arrhenius plots determined for grain boundary self diffusion of Zn [27], and DP and DCI in an earlier study by the present authors [14] have been reproduced in Fig. 9. It is apparent from the slopes of the plots that the Livingston–Cahn model would lead to a lower value of Q_b compared to that from the other lines. Table III presents a comparison of the Q_b and $(s\delta D_b)_o$ values calculated from the different plots in Fig. 9.

4. Summary and conclusions

1. Isothermal ageing in the Zn–4 at % Ag in the range 353–513 K following DP at 393 K for 60 h leads to type II discontinuous coarsening (DCII) of the primary precipitation products (i.e. DP).

2. The interfaces between two former DP colonies seem to be the preferential initiation sites for DCII.

3. A 1–2 μm thick precipitate-rich envelope which develops during coarsening reaction induces an incoherent character capable of undergoing thermally activated migration, and allows DCII initiation either from one or from both sides of the same interface between two former DP colonies.

4. The precipitate lamellae in the DCII colonies do not bear any strict orientation relationship with those in the DP colonies being consumed.

5. λ_{DCII} is comparable to λ_{DCI} up to 433 K, following which $\lambda_{DCII} > \lambda_{DCI}$. However, λ_{DCII} (also λ_{DCI}) is

TABLE II Kinetic data of DCII following DP at 393 K for the estimation of $(s\delta D_b)$ as a function of T through Equations 6 and 7

T (K)	v ($m\,s^{-1}$)	λ_{DCII} (μm)	ΔG_{DCII} ($J\,mol^{-1}$)	$(s\delta D_b)_{L-C}$ ($m^3\,s^{-1}$)	$(s\delta D_b)_{P-H}$ ($m^3\,s^{-1}$)
353	3.3×10^{-12}	1.62	−29.6	1.3×10^{-21}	1.1×10^{-22}
393	1.5×10^{-11}	1.78	−15.5	3.3×10^{-21}	1.2×10^{-21}
413	3.8×10^{-11}	1.70	−11.1	5.9×10^{-21}	4.2×10^{-21}
433	7.5×10^{-11}	2.11	−10.0	1.3×10^{-20}	1.5×10^{-20}
453	6.7×10^{-11}	2.10	−9.0	9.3×10^{-21}	1.5×10^{-20}
513	5.4×10^{-10}	2.02	−19.6	3.4×10^{-20}	6.0×10^{-20}

(The subscripts L–C and P–H refer to the respective models [4] and [25])

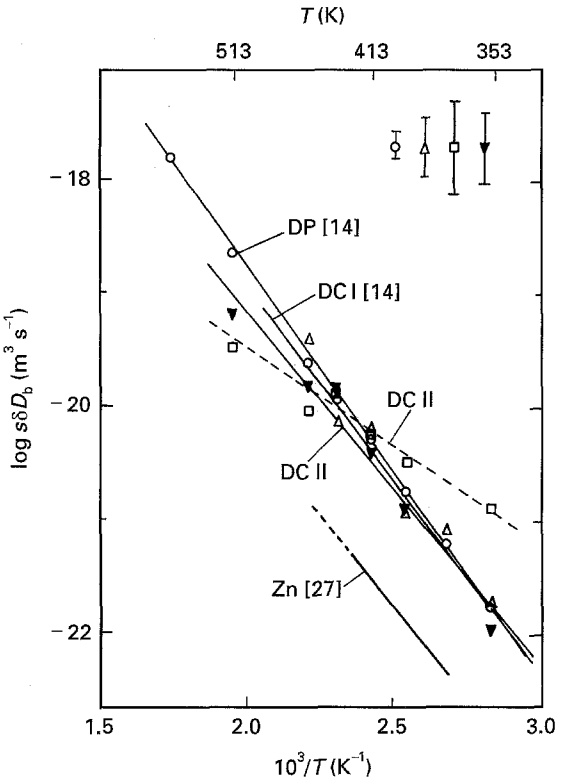

Figure 9 Arrhenius plot of $s\delta D_b$ for DP [14], DCI [14] and DCII obtained as per the modified Petermann–Hornbogen model [25]. A similar plot for boundary self diffusion of Zn is included for comparison. The broken line represents the Arrhenius plot for DCII derived from the Livingston–Cahn model [4].

4–6 times larger than λ_{DP} at a comparable stage of coarsening.

6. v_{DCII} is marginally higher than v_{DCI}, but 1–2 orders of magnitude smaller than v_{DP} at a given temperature.

7. The activation energy for boundary diffusion (Q_b) determined in this study through kinetic analysis of DCII using the modified Petermann–Hornbogen model are comparable with the same obtained from an earlier DP and DCI study, and also for grain boundary self diffusion in Zn. The Q_b values are nearly 50% of the activation energy for volume diffusion (Q_v) of Ag in Zn.

8. The Q_b value obtained from the Livingston–Cahn model is unusually low because of an under estimation of the driving force (due to neglecting the chemical free energy changes in DCII), and hence, is not acceptable.

9. Considering the Q_b values obtained in this study, DCII seems to be a boundary diffusion controlled process in this alloy.

Acknowledgements

The partial financial support from the Council of Scientific and Industrial Research (Grant No. 10/147/91/ EMR-II) and equipment support from the Board of Research for Nuclear Sciences (Grant No. 34/7/89-G) are gratefully acknowledged.

References

1. M. FRIESEL, I. MANNA and W. GUST, *J. Phys. (Colloque)* **51** (1990) C1-381.
2. R. D. DOHERTY, in "Physical Metallurgy", edited by R. W. Cahn and P. Hansen (North-Holland Physics, Amsterdam, 1983) p. 996.
3. I. KAUR and W. GUST, in "Fundamentals of Grain and Interphase Boundary Diffusion" (Ziegler Press, Stuttgart, 1989) p. 232.
4. J. D. LIVINGSTON and J. W. CAHN, *Acta Metall.* **22** (1974) 495.
5. C. P. JU and R. A. FOURNELLE, *ibid.* **33** (1985) 71.
6. V. SURESH and S. P. GUPTA, *Z. Metallkde* **77** (1986) 529.

TABLE III Comparison of Arrhenius parameters of grain boundary chemical diffusion of Ag in Zn–Ag determined through kinetic analysis of DCII [this study] and DP/DCI [14]

	Model	$(s\delta D_b)_0$ ($m^3\,s^{-1}$)	Q_b ($kJ\,mol^{-1}$)	Q_b/Q_v
DP[a]	Petermann–Hornbogen [26]	2.3×10^{-12}	68.2	0.61
DCI[a]	Modified Petermann–Hornbogen [25]	2.8×10^{-12}	66.2	0.59
DCII	Modified Petermann–Hornbogen [25]	1.7×10^{-13}	61.0	0.54
DCII	Livingston–Cahn [4]	4.5×10^{-17}	30.7	0.27
Grain boundary self diffusion in Zn [27]		1.9×10^{-14}	61.1	0.55
Tracer impurity diffusion of Ag^{110} in Zn [28]		3.9×10^{-5}	112.0	1.00

[a](Obtained from [14])

7. S. P. GUPTA, *ibid.* **77** (1986) 472.
8. T. H. CHUANG, R. A. FOURNELLE, W. GUST and B. PREDEL, *Acta Metall.* **36** (1988) 775.
9. V. V. BALASUBRAHMANYAM and S. P. GUPTA, *ibid.* **37** (1989) 291.
10. H. TSUBAKINO, R. NAZATO and A. YAMAMOTO, *Mater. Sci. Tech.* **9** (1993) 288.
11. *Idem, J. Mater. Sci.* **26** (1991) 2851.
12. J. W. CAHN, *Acta Metall.* **7** (1959) 18.
13. M. SHAARBAF and R. A. FOURNELLE, *Mater. Sci. Eng.* **102A** (1988) 271.
14. I. MANNA, J. N. JHA and S. K. PABI, *Acta Metall. Mater.* (communicated).
15. R. LÜCKE, *Z. Metallk.* **66** (1975) 448.
16. I. MANNA, S. K. PABI and W. GUST, *Acta Metall. Mater.* **39** (1991) 1489.
17. M. FREBEL and SCHENK, *Z. Metallkde* **70** (1979) 230.
18. I. MANNA and S. K. PABI, *J. Mater. Sci. Lett.* **9** (1990) 554.
19. I. MANNA, J. SWAMINATHAN and S. K. PABI, *Z. Metallkde* **85** (1994) 50.
20. R. A. SWALIN, in "Thermodynamics of Solids" (John Wiley & Sons, Inc., New York, 1962) p. 102.
21. R. HULTGREN, R. L. ORR, P. D. ANDERSON and K. K. KELLEY, "Selected Values of Thermodynamic Properties of Metals and Alloys" (John Wiley & Sons, Inc. New York, 1963) p. 397.
22. L. E. MURR, "Interfacial Phenomena in Metals and Alloys" (Addison-Wesley, London, 1975) p. 133.
23. G. B. GIBBS, *Phys. Status Solidi* **16** (1966) K27.
24. M. HANSEN and K. ANDERKO, in "Constitution of Binary Alloys" (McGraw Hill, New York, 1958) p. 63.
25. R. A. FOURNELLE, *Acta Metall.* **27** (1979) 1135; **27** (1979) 1147.
26. J. PETERMANN and E. HORNBOGEN, *Z. Metallkde* **59** (1968) 824.
27. E. S. WAJDA, *Acta Metall.* **2** (1954) 184 [cited after I. Kaur, W. Gust and L. Kozma, "Handbook of Grain and Interphase Boundary Diffusion Data", Vol. 2 (Ziegler Press, Stuttgart, 1989) p. 1416].
28. J. H. ROSOLOWSKI, *Phy. Rev.* **124** (1961) 1828.

Received 12 January
and accepted 19 September 1995